Journal of the Korean Nuclear Society
Volume 21, Number 4, December, 1989

Development of Axial Power Distribution Monitoring System Using Two-Level Excore Detector

Sung-Goo Chi, Jae-Woong Song, Dwak-Hwan Ahn, Jung-Eui Kuh
Korea Advanced Energy Reserch Institute
(Received August 21, 1989)

상하부 2개의 노외계측기를 이용한 축방향 출력분포 감시계통 개발

지성구, 송재웅, 안덕환, 구정의
한국에너지연구소
(1989. 8. 21 접수)

Abstract

The Axial Power Distribution Monitoring System(APDMS) program was developed to calculate a detailed axial power distribution using two-level excore detector, cold leg temperature and control rod position signals. The unnormalized two-level excore detector signals were corrected for the rod shadowing factor determined by control rod position and for the temperature shadowing factor calculated based on cold leg temperature. A shape annealing matrix was then applied to the corrected excore detector response to yield peripheral power. After the core average power was obtained using linear relationship between core average and peripheral power, the boundary point power correction coefficient was applied to core average power in order to obtain boundary power for both upper and lower core axial boundaries. Then, the axial power distribution was synthesized by spline approximation. In spite of burnup, power level, control rod postion and axial offset changes, the comparisons of axial power distributions between BOXER simulation program and APDMS results showed good agreements within 5% root mean square error for Kori Unit 3 Cycle 4.

요 약

상하부 2개의 노외계측기, 노입구관 온도 및 제어봉 위치 신호를 이용하여 상세한 축방향 출력분포를 계산할 수 있는 APDMS 프로그램을 개발하였다. 상하부 2개의 노외계측기 신호가 제어봉 위치에 의하여 결정된 제어봉 간섭계수와 노입구관 온도에 따른 온도 간섭계수에 대하여 보정된 후 노심 주변출력을 얻기 위하여 보정된 노외계측기 신호에 shape annealing matrix가 적용되었다. 노심의 상하부 경계에서의 출력을 얻기 위해서는 평균 노심출력과 주변출력과의 선형적 관계를 이용한 노심 상하부의 평균출력에 경계점 출력보정계수가 적용되었다. 축방향 출력분포가 2개의 노외계측기에 의해 계산된 상하부 평균 노심출력, 상하부 경계

면에서의 출력 및 미리 계산된 노심의 중심 위치에서의 출력을 이용하여 spline approximation에 의하여 계산되었다. 연소도, 출력준위, 제어봉 위치 및 axial offset의 변화에도 불구하고 고리 3호기 4주기에 대하여 BOXER 코드와 APDMS 프로그램에 의해 계산된 축방향 출력분포의 비교는 5% root mean square 오차내에서 일치함을 보여 주었다.

1. Introduction

Axial power distribution control is at the heart of any nuclear power plant operation. Yet, the operating plants in Korea rely on a technology developed 20 and 30 years ago to perform this vital function. Available information on axial power distribution often lacks detailed and real-time characteristics needed to operate the plant as efficient as possible. Lack of accurate and real-time axial power distribution data not only leads to reduced capacity factor, but also results in inefficient core control strategies and procedures that increase operating costs and replace additional duties on the operating staff.

Currently, the detailed axial power distribution is not directly measurable for the nuclear power plant with a two-level excore detector system such as Westinghouse designed Korean Nuclear Units. Only excore and incore axial offsets(AO) are calculated as a gross axial power indication of top and bottom half using two-level excore system to monitor and control reactor core. Therefore, axial power control in these units is performed on a trial and error basis with only AO information. Experience can be a strong influence, but lesson learned in the past may not be applicable to the current fuel burnup. Also, because the operator does not normally have a reliable analytical tool to support axially oriented core control, it sometimes leads to an over-reliance on and overly conservative use of reactor coolant system boron concentration change. This practice results in the production of larger quantities of reactor coolant effluent which m;ust be subsequently processed and which, under end of cycle condition, could lead to restrictions in plant maneuverablity.

In order to overcome these difficulties, a preliminary study was performed by developing Axial Power Distribution Monitoring System (APDMS) program to calculate detailed axial power distribution for at least twenty axial nodes. The axial power distribution is synthesized using two-level excore detector, cold leg temperature and control rod position.

This on-line, real-time detailed axial power monitoring can support to quantify current core behavior for direct comparison to limiting conditions for operation. In addition, such a system can supersede the need of technical specifications that infer potentially unacceptable core power distribution.

2. Calculation Method

The core average axial power distribution is calculated using input from two-level excore detector, cold leg temperature and control rod position signal. The unnormalized two-level excore signals are corrected for the rod shadowing factor(RSF) determined by control rod position and for the temperature shadowing factor(TSF) calculated based on cold leg temperature(Tcold). A shape annealing matrix(SAM) is then applied to the corrected excore detector response to yield peripheral power. After the core average power is obtained using linear relationship between core average and peripheral power, the boundary point power correction coefficient(BPPCC) is applied to core average power in order to obtain boundary power for both upper and lower core

axial boundaries. Then, the axial power distribution is synthesized by solving a set of simultaneous equation in which the power distribution is approximated by a set of piecewise continuous cubic polynomials called spline function[1].

The overall calculation procedure to obtain axial power distribution is shown in Figure 1. The

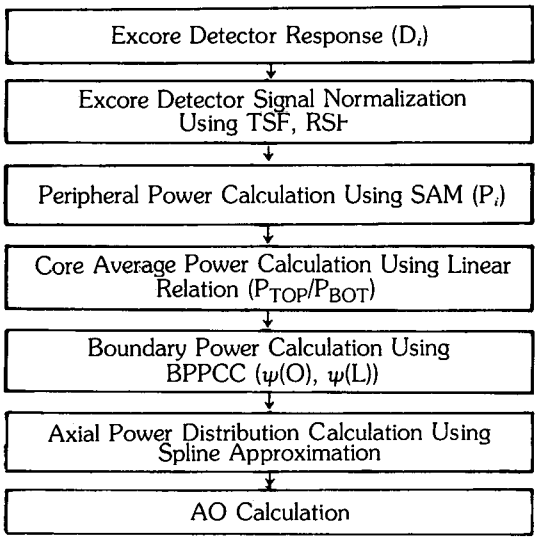

Fig. 1. Axial Power Distribution Calculation Procedure

detailed calculation method is described as below.

The RSF is used to account for the alternation in fast neutron flux seen by the excore detectors when control rods are inserted assuming no change in gross power level. The excore detector responses are corrected by dividing the RSF in accordance with control rod insertion in the core. The RSFs were calculated using excore detector response changes by control rod insertion as follow:

$$RSF_n = \frac{\sum_{i=1}^{2} D_i^n}{\sum_{i=1}^{2} D_i(ARO)} \qquad i=1,2$$

where, D is unnormalized excore detector response.

n = 1 is control bank CD in.

n = 2 is control bank CD + CC in.

n = 3 is control bank CD + CC + CB in.

The TSF is used to adjust the excore detector response for change in Tcold. The temperature variation in Tcold is accompanied by water density change across the downcomer region of reactor vessel, which affects neutron attenuation, and therefore, excore detector response. The excore detector signal is corrected by multiplying the TSF in accordance with the Tcold variation from the nominal value. The TSF was calculated by producing the best estimate of the excore detector response variation as a function of Tcold as shown in Figure 2. The slope of the resulting from a least square fit is the estimated TSF.

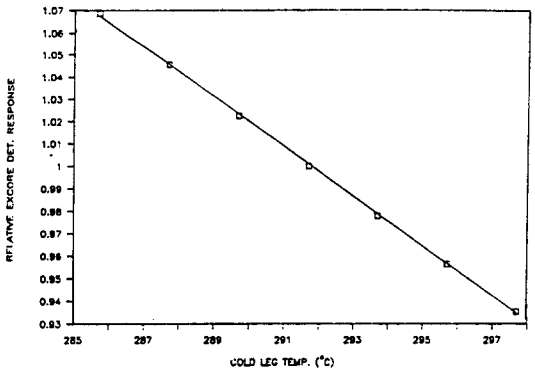

Fig. 2. Excore Detector Response Change as a Function of Tcold

Because each excore detector responds to entire axial extent of core but responds most to fast neutron from peripheral assemblies neasrest to them, shape annealing correction of detector responses is required to synthesize an average axial power distribution. The SAM is utilized to

calculate the core peripheral power from the ex-core detector response as follow:

$$P_i = \sum_{j=1}^{2} S_{ij} D_j \qquad i=1,2$$

where, P_i is peripheral power of top and bottom half, respectively.

D_i is corrected excore detector response from top and bottom half, respectively.

S_{ij} is SAM for flux at detector i due to flux at core peripheral in the jth core region.

The relationship between core average and peripheral power is needed to obtain the boundary power. An investigation of the peripheral and average power for a large range of AO change shows linear relationship between them as shown in Figure 3.

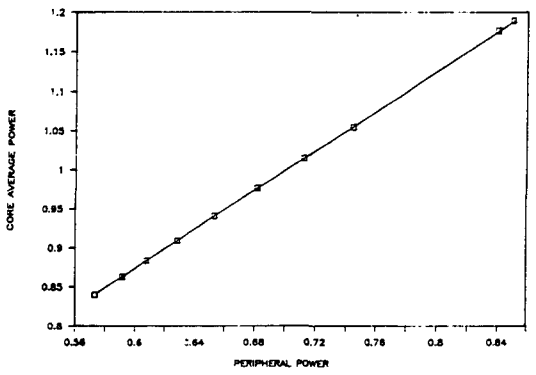

Fig. 3. Relationship Between Core Average nd Peripheral Power

The synthesis of axial power distribution requires the power for both top and bottom at boundary, which is calculated based on the core average power in each region as follows:

$$\psi(0) = BPPCC3 \times P_{TOP} + BPPCC4$$
$$\psi(L) = BPPCC1 \times P_{BOT} + BPPCC2$$

where, P_{TOP} and P_{BOT} are core average power in top and bottom half.

$\psi(0)$ and $\psi(L)$ are power at upper and lower core axial boundary.

The SAM and BPPCC values were calculated by a least square fitting relating calculated values of P_i and D_i during an induced free xenon oscillation as shown in Figure 4. The mean squre error is

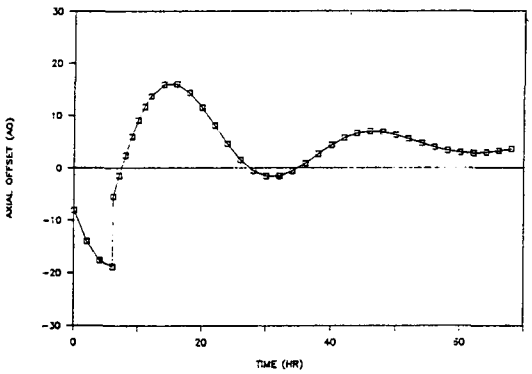

Fig. 4. Induced Free Xenon Oscillation at 75% Power

$$e_i^2 = (P_i - S_{i1}D_1 - S_{i2}D_2)^2 \qquad i = 1,2$$

The best values of S_{ij} occur when $\frac{\delta e_i^2}{\delta S_{ij}} = 0$

It yields

$$\begin{bmatrix} S_{i1} \\ S_{i2} \end{bmatrix} = \begin{bmatrix} \langle D_1^2 \rangle & \langle D_1 D_2 \rangle \\ \langle D_2 D_1 \rangle & \langle D_2^2 \rangle \end{bmatrix}^{-1} \begin{bmatrix} \langle P_i D_1 \rangle \\ \langle P_i D_2 \rangle \end{bmatrix}$$

where, $<\rho>$ is defined as $\frac{1}{N}\sum_{i=1}^{N}\rho^{i}$

N is number of data sets obtained during free xenon oscillation.

Similarly, the best values of BPPCC can be obtained as follows:

$$\begin{bmatrix} BPPCC3 \\ BPPCC4 \end{bmatrix} = \begin{bmatrix} <P_{TOP}P_{TOP}> & -<P_{TOP}> \\ -<P_{TOP}> & 1 \end{bmatrix}^{-1} \begin{bmatrix} <P_{TOP}\,\psi(0)> \\ -<\psi(0)> \end{bmatrix}$$

$$\begin{bmatrix} BPPCC1 \\ BPPCC2 \end{bmatrix} = \begin{bmatrix} <P_{BOT}P_{BOT}> & -<P_{BOT}> \\ -<P_{BOT}> & 1 \end{bmatrix}^{-1} \begin{bmatrix} <P_{BOT}\,\psi(L)> \\ -<\psi(L)> \end{bmatrix}$$

The normalized core average axial power distribution is calculated by the combinations of cubic basis functions which can be solved simultaneously for five unknown coefficients. Those five points are two power levels calculated by excore detector response, two power levels at core upper and lower axial boundaries, and the power at core center location.

3. Results and Discussions

Table 1 provides TSF, RSF, SAM, BPPCC and core average and peripheral power relationship for Kori Unit 3 Cycle 4 calculated by BOXER[2] and IQSBOX[3,4] simulation codes. First, the power at center location was investigated in order to synthesize axial power distribution. The power at center location was linearly decreased as a function of burnup as shown in Figure 5. This

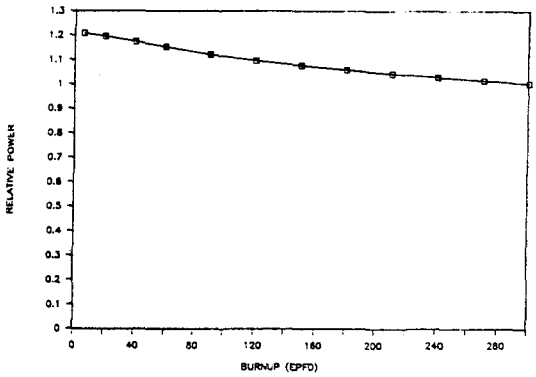

Fig. 5. Power Change at Center Location as a Function of Core Life

is expected, since a cosine shaped axial power distribution migrates over core life to a saddle shaped power distribution as shown in Figure 6.

Table 1. Parameters for Axial Power Distribution Calculation for Kori Unit 3 Cycle 4

Parameter	Values			
TSF	.011125			
RSF	CD In .98214	CD+CC In .95912	CD+CC+CB In .9775	
SAM	S11 .030715	S12 -.003233	S21 -.001497	S22 .029849
Slope Intercept	.261516 .117080			
BPPCC	BPPCC1 .501738	BPPCC2 .139838	BPPCC3 .628494	BPPCC4 .270429

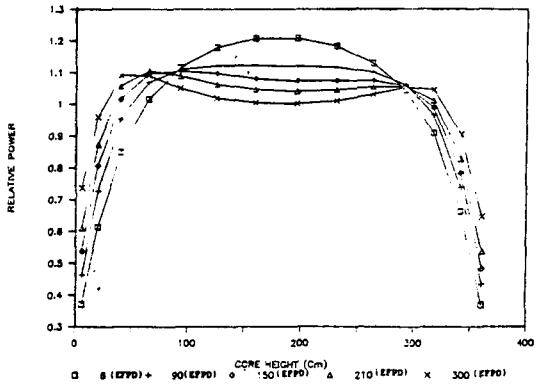

Fig. 6. Axial Power Distribution Change as a Function of Core Life

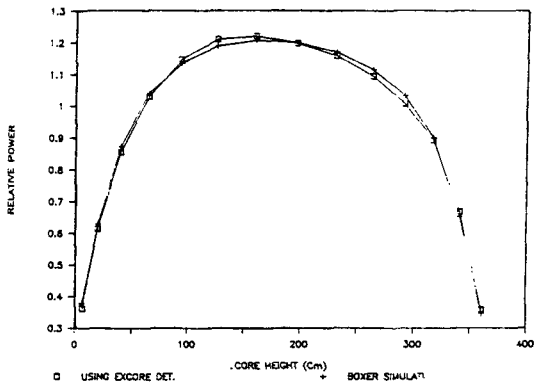

Fig. 7. Axial Power Distribution Comparison for Case 1

The change in center location response from it's nominal value due to xenon oscillation was less than 5% as shown in Table 2.

Table 2. Center Location Response as a Function of Core Life and Axial Offset for Unit 3 Cycle 4

Condition	BOC	MOC	EOC
Equilibrium AO	-.5700	-2.054	-2.022
Center Location Response	1.2082	1.0765	1.0237
Minimum AO	18.976	-25.37	-28.13
Center Location Response	1.1902	1.0354	.9706
Change from Equiliium	1.490%	3.818%	5.180%
Maximum AO	15.999	22.343	25.308
Center Location Response	1.2027	1.0717	1.0299
Change from Equilibrium	.455%	.446%	-.606%

Table 3. APDMS Calculation Results

Case	Burnup	Power (%)	Rod Position	BOXER AO (%)	Calculated AO (%)	RMS error (%)
1	BOC	100	ARO	-1.882	-.5015	1.564
2	BOC	30	ARO	14.44	15.1448	3.484
3	BOC	75	110 step	-18.976	-17.976	2.273
4	EOC	75	ARO	1.332	2.1064	3.275
5	EOC	75	ARO	15.677	18.1693	3.697
6	EOC	75	110 step	-20.798	-22.798	4.654

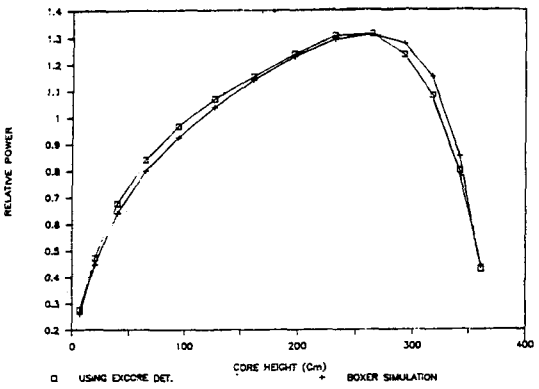

Fig. 8. Axial Power Distribution Comparison for Case 2

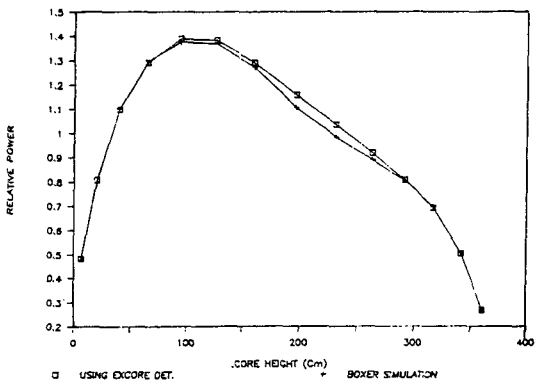

Fig. 9. Axial Power Distribution Comparison for Case 3

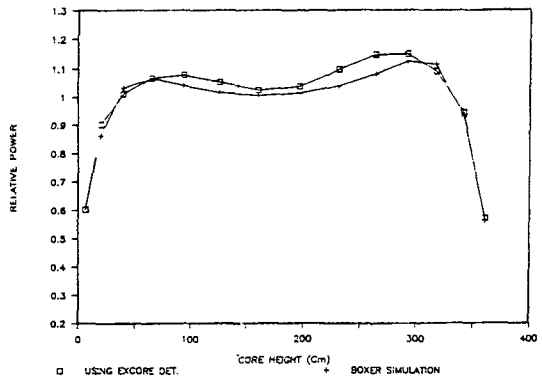

Fig. 10. Axial Power Distribution Comparison for Case 4

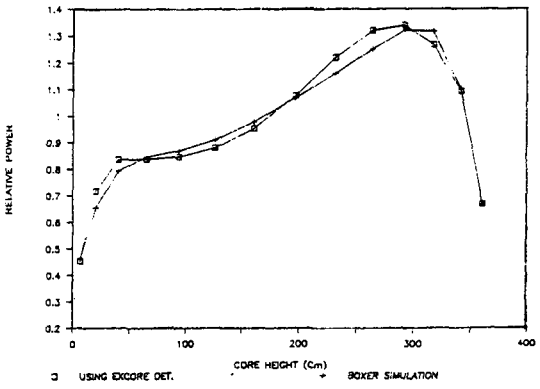

Fig. 11. Axial Power Distribution Comparison for Case 5

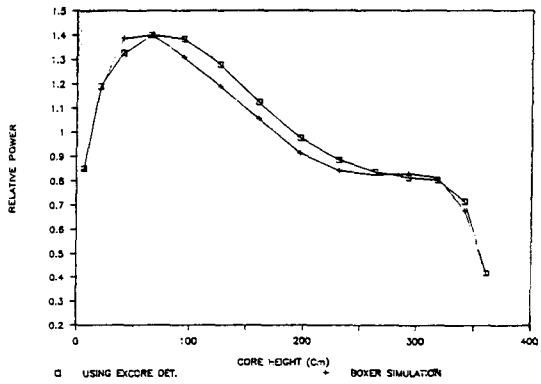

Fig. 12. Axial Power Distribution Comparison for Case 6

Figures 7,8,9,10,11 and 12 provide comparisons of axial power distributions calculated by BOXER simulation code and APDMS program. The axial power distributions were calcualted at 14 nodes for the purpose of comparison with simulation code as a function of burnup, power level, control rod position and AO. It is pointed out that the values of AO analyzed are very extreme, and would not be encountered on normal operating situation. Nonetheless, every cases showed good agreements within 5% root mean square(RMS) error range as shown in Table

3.

For practical implementation to an operating nuclear power plant which has only two-level ex-core detector system, the following activities are additionally required.

1) The startup test should be performed to measure plant and cycle specific SAM and BPPCC etc. at each reload.
2) The relative power at center location should be updated by monthly base as an user input. This can be performed by obtaining full core flux mapping at 100% power and all rod out condition as required by technical specification.
3) A minor hardware change is necessary for connecting excore dtector signal, cold leg temperature and control rod position to a plant computer or personal computer through the analog to digital converter.

References

1. S.D. Conte and Carl de Boor, "Elementary Numerical Analysis", 289, McGraw-Hill, New York (1980).
2. R. Boeer, H. Finnemann and M. Voigh, "Code Manual BOXER 8.6", Tecnical Report ST 1/ST114/87/e314, (1987).
3. H. Finnemann and W. Gundlach, "Space Time Kinetics Code IQSBOX for PWR and BWR, Part I: Description of Physical and Thermo-hydraulic Methods," Atomkernenergic/Kerntechnik, 37, 176-183 (1981).
4. R. Boer, H. Finnemann, M.Gruner and R. Muller, "Code Manual IQSBOX 8.7", ST 1/ST114/87/e315a, (1987).